Limnol. Oceanogr., 50(2), 2005, 493–507

Testing the direct effect of CO_2 concentration on a bloom of the coccolithophorid *Emiliania huxleyi* in mesocosm experiments

Anja Engel
Alfred Wegener Institute for Polar and Marine Research, 27515 Bremerhaven, Germany; Marine Sciences Research Centre, State University of New York at Stony Brook, Stony Brook, New York 11740

Ingrid Zondervan
Alfred Wegener Institute for Polar and Marine Research, 27515 Bremerhaven, Germany

Katrien Aerts
Department of Chemistry, University of Antwerp, 2610 Wilrijk, Belgium

Luc Beaufort
CNRS, 13545 Aix-en-Provence cedex 4, France

Albert Benthien
Alfred Wegener Institute for Polar and Marine Research, 27515 Bremerhaven, Germany; Woods Hole Oceanographic Institution, Department of Geology and Geophysics, Woods Hole, Massachusetts 02543

Lei Chou
Océanographie Chimique et Géochimie des Eaux, Université Libre de Bruxelles, 1050 Brussels, Belgium

Bruno Delille
Unité d'Océanographie Chimique, MARE, Université de Liège, 4000 Liège, Belgium

Jean-Pierre Gattuso
Laboratoire d'Océanographie de Villefranche, CNRS-UPMC, 06234 Villefranche-sur-mer cedex, France

Jerome Harlay
Océanographie Chimique et Géochimie des Eaux, Université Libre de Bruxelles, 1050 Brussels, Belgium

Christel Heemann and Linn Hoffmann
Alfred Wegener Institute for Polar and Marine Research, 27515 Bremerhaven, Germany

Stéphan Jacquet
UMR CARRTEL, Station INRA d'Hydrobiologie Lacustre, 74203 Thonon-les-Bains cedex, France

Jens Nejstgaard
Department of Fisheries and Marine Biology, University of Bergen, 5020 Bergen, Norway

Marie-Dominique Pizay
Laboratoire d'Océanographie de Villefranche, CNRS-UPMC, 06234 Villefranche-sur-mer cedex, France

Emma Rochelle-Newall
Laboratoire d'Océanographie de Villefranche, CNRS-UPMC, 06234 Villefranche-sur-mer cedex, France; Centre IRD de Noumea, BPA5, 98848, Noumea, New Caledonia

Uta Schneider and Anja Terbrueggen
Alfred Wegener Institute for Polar and Marine Research, 27515 Bremerhaven, Germany

Ulf Riebesell
Alfred Wegener Institute for Polar and Marine Research, 27515 Bremerhaven, Germany; Leibniz Institut für Meereswissenschaften, University at Kiel, 24105 Kiel, Germany

Abstract

We studied the direct effects of CO_2 and related changes in seawater carbonate chemistry on marine planktonic organisms in a mesocosm experiment. In nine outdoor enclosures (~11 m^3 each), the partial pressure of CO_2 (pCO_2) in the seawater was modified by an aeration system. The triplicate mesocosm treatments represented low (~190 parts per million by volume (ppmV) CO_2), present (~410 ppmV CO_2), and high (~710 ppmV CO_2) pCO_2 conditions. After initial fertilization with nitrate and phosphate a bloom dominated by the coccolithophorid *Emiliania huxleyi* occurred simultaneously in all of the nine mesocosms; it was monitored over a 19-day period. The three CO_2 treatments assimilated nitrate and phosphate similarly. The concentration of particulate constituents was highly variable among the replicate mesocosms, disguising direct CO_2-related effects. Normalization of production rates within each treatment, however, indicated that the net specific growth rate of *E. huxleyi*, the rate of calcification per cell, and the elemental stoichiometry of uptake and production processes were sensitive to changes in pCO_2. This broad influence of CO_2 on the *E. huxleyi* bloom suggests that changes in CO_2 concentration directly affect cell physiology with likely effects on the marine biogeochemistry.

Large-scale changes in surface ocean chemical equilibrium and elemental cycling have occurred in the ocean's history and are expected to continue and intensify in the future. Prior to the industrial burning of fossil fuels, CO_2 concentration varied between 180 and 280 parts per million by volume (ppmV), with the lower values observed during glacial times. Since the middle of the 18th century, the atmospheric partial pressure of CO_2 (pCO_2) has increased rapidly from 280 to 366 ppmV in 1998, and several future scenarios predict a further increase to 750 ppmV in 2100 (IPCC scenario IS92a; Houghton et al. 2001). The progressive increase in atmospheric CO_2 might affect the marine biosphere directly and indirectly. Indirect effects are expected through rising sea surface temperatures related to global warming, which might cause increased surface ocean stratification and mixed layer insulation and could also affect the rates of biological processes. Moreover, the increase of atmospheric temperature will likely modify global wind patterns, subsequently changing the dust input and the iron supply to the surface ocean.

Because of the rapid air–sea exchange of CO_2, direct, and already determined, effects of increased atmospheric CO_2 concentration are the rise of CO_2 concentration in the surface ocean and a related shift in its chemical equilibrium (Chen and Millero 1979; Brewer et al. 1997). Several species of dissolved inorganic carbon (DIC) exist in seawater, namely CO_2, HCO_3^-, and CO_3^{2-}, the proportions of which are largely determined by the total DIC concentration, pH, and total alkalinity (TA). TA is defined as the number of moles of $[H^+]$ equivalent to the excess of proton acceptors per kilogram of seawater (Dickson 1981). At typical seawater pH of 8.2, about 90% of DIC is present as HCO_3^-, 9% as CO_3^{2-}, and <1% as CO_2. When DIC increases through enhanced uptake of CO_2 from the atmosphere, the pH of seawater and the CO_3^{2-} concentration decrease. The expected decrease in surface ocean pH by 0.7 units up to the year 2300 will exceed anything experienced in the past 300,000 yr of earth history (Caldeira and Wickett 2003).

This change of environmental factors is likely to affect the physiology of marine organisms and therefore has the potential to influence species composition and competition, as well as the cycling of biogeochemical key elements, such as C, N, and P.

Marine phytoplankton might be particularly sensitive to CO_2-related changes in the carbonate chemistry because inorganic carbon assimilation is largely bound to CO_2 fixation by the carboxylating enzyme, ribulose-1,5-bisphosphate carboxylase/oxygenase, which has a low affinity to CO_2 with half-saturation constants ranging between 30 and 70 μmol L^{-1} (Badger et al. 1998). Many phytoplankton species are able to enhance their CO_2 supply to the site of carboxylation by CO_2 concentrating mechanisms (CCMs; Raven 1991, e.g., through active uptake of HCO_3^- or the enhancement of HCO_3^-, or both) to CO_2 conversion with the enzyme carbonic anhydrase (CA). Operation of the CCMs thereby ensures that photosynthetic carbon fixation is close to saturating primary production, even at the low CO_2 concentrations typically encountered in the surface ocean (i.e., 8–22 μmol L^{-1}; Goerike and Fry 1994). However, an increase of CO_2 concentration might reduce the need for CCM activity and thereby lower the metabolic costs of the phytoplankton cells for inorganic carbon acquisition. Moreover, recent studies demonstrated that phytoplankton species and functional groups differ regarding the efficiency and regulation of their CCMs, indicating that changes in CO_2 availability might affect competition and succession of phytoplankton species (Burkhardt et al. 2001; Rost et al. 2003). A significant shift in the taxonomic composition of a phytoplankton assemblage exposed to different CO_2 levels was indeed observed in a recent study by Tortell et al. (2002). Differences in CO_2 uptake rates were further hypothesized to influence the production of extracellular organic matter, as demonstrated by the increase of transparent exopolymer particle (TEP) concentration with CO_2 concentration in an experimental study conducted with Baltic Sea phytoplankton (Engel 2002). The origination of

Acknowledgments

We are grateful to the staff of the Large Scale Facility (LFS) in Bergen, Norway, in particular to Clelia Booman, Jorun Egge, Agnes Aadnesen, and Erling Heggoy, who gave us a warm welcome and helped us accomplish our study. Kai Buss and Michael Schlüter from the IUV were significantly involved in the development of the experimental setup. Erich Dunker and Martha Stürcken-Rodewald are acknowledged for technical support. Christoph Völker, Silke Thoms, and Markus Schartau provided fruitful discussions.

This work was supported by the Alfred Wegener Institute for Polar and Marine Research and the European Commission Human Potential Programme HPRI-1999-0056. Additional support was provided by European Union project EUROTROPH (EVK3-CT-2000-00040), a Marie Curie fellowship (HPMF-CT-1999-00030), and the Belgian Federal office for Scientific, Technical, and Cultural affairs (EV/11/5A).

TEPs from dissolved organic matter could indicate that the partitioning between the dissolved and the particulate organic carbon pool is sensitive to changes in CO_2 concentration.

A strong effect of CO_2-related changes in the carbonate chemistry of seawater was recently demonstrated for calcification by marine phytoplankton. In laboratory experiments with nutrient-replete cultures of the marine coccolithophorids *Emiliania huxleyi* and *Gephyrocapsa oceanica*, it was shown that the ratio of particulate inorganic carbon (PIC) to particulate organic carbon (POC) production decreased with increasing CO_2 concentration (Riebesell et al. 2000; Zondervan et al. 2001, 2002). The change in [PIC] : [POC] ratios was attributed to a decrease in calcification rates, as well as an increase in organic carbon production. In nitrate-limited cultures of *E. huxleyi*, however, such a change in the ratio of calcification to organic carbon production was not observed (Sciandra et al. 2003). Together with foraminifera and corals, coccolithophorids are the major producers of calcium carbonate in the ocean. Because calcium carbonate formation is a chemical reaction that liberates CO_2 (i.e., $Ca^{2+} + 2\ HCO_3^- \rightarrow CaCO_3 + CO_2 + H_2O$), the response of reduced calcification might provide a significant negative feedback to increasing CO_2 concentration.

Hence, CO_2-related effects on the physiology of marine phytoplankton have the potential to affect carbon cycling by affecting both the rate of organic carbon assimilation and the amount of biological calcification. On a global scale, these effects could translate into changes in the efficiency of the biological carbon pumps—specifically, the soft tissue and carbonate pumps—and potentially affect global carbon sequestration (e.g., through changing of the ''rain ratio'' of PIC and POC). Because it has been proposed that the soft tissue pump is ultimately determined by the availability of inorganic nutrients, specifically nitrate (Dugdale and Goering 1967; Eppley and Peterson 1979), a CO_2-related change of organic carbon sequestration would require a CO_2 effect on the C : N stoichiometry of the sinking particles. Apart from a few laboratory experiments, which indeed demonstrated a CO_2 effect on the stoichiometry of phytoplankton cells (Burkhardt et al. 1999; Gervais and Riebesell 2001; Urabe et al. 2003), it is still unknown whether CO_2 changes cause a systematic shift in the C : N : P stoichiometry of export production. From the potential linkages mentioned above, it is, however, evident that a mechanistic understanding of the influence of CO_2 effects on marine phytoplankton and of the consequences for biogeochemical cycling is essential to reliably assess ecosystem changes and the future concentration of CO_2 in the atmosphere.

To study the response of a natural phytoplankton bloom to different CO_2 concentrations, we designed an experimental, semienclosed system that enables the modification of seawater CO_2 concentration without changing TA, while maintaining an environment as natural as possible. Here, we present the setup of the experiment and give an overview on the development and biogeochemistry of a bloom of the marine coccolithophorid *E. huxleyi*, which developed during the exposure to three different CO_2 concentrations.

Materials and methods

Setup and sampling—The study was conducted between 31 May and 25 June 2001 at the European Union Large Scale Facility (LSF) in Bergen, Norway. Nine polyethylene enclosures (~11 m^3, 4.5 m water depth) were moored to a raft in the Raunefjorden (60.3°N, 5.2°E; for more details, see Williams and Egge 1998). The enclosures were filled with unfiltered, nutrient-poor, postbloom fjord water, which was pumped from 2 m depth adjacent to the raft. The enclosures were covered by gas-tight tents made of ethylene tetrafluoroethylene foil (Foiltec, Bremen, Germany), which allowed for 95% light transmission of the complete spectrum of sunlight, including ultraviolet A (UVA) and UVB.

The atmospheric and seawater pCO_2 were manipulated to achieve three different CO_2 levels in triplicate: (1) high pCO_2, approximately simulating the atmospheric CO_2 concentration in year 2100 (mesocosms 1–3), representing IPCC's ''business as usual'' scenario IS92a; (2) present pCO_2 (mesocosms 4–6), representing the present day environment; and (3) low pCO_2 (mesocosms 7–9), representing the glacial atmosphere. The setup of the experimental system was designed by the Institute for Environmental Process Engineering (IUV, Bremen, Germany) and is displayed in Fig. 1. With the use of rotary vane compressors (Becker, DT-4.8) different CO_2 levels in seawater were achieved by aerating the water and fumigating the tents with air enriched with either pure CO_2 (pureness 2.7), natural air, or air depleted in CO_2. The latter was obtained by running natural air through a CO_2 absorber (Na_2CO_3 platelets with a pH indicator). After 4 d of CO_2 adjustment, the desired pCO_2 levels in water were reached (day 0) and the CO_2 aeration of the water column was stopped.

To promote the development of a coccolithophorid bloom, $NaNO_3$ and Na_2HPO_4 were added on day 0 (6 June 2001) at a ratio of 30 : 1, yielding initial concentrations in the seawater of 15.3 μmol L^{-1} nitrate and 0.5 μmol L^{-1} phosphate. After nutrient addition and throughout the study, the water was gently mixed by means of an airlift (for more details, see Egge and Asknes 1992) with the same air as for gassing the tents. The gassing of the tents was continued to keep the pCO_2 of the overlying atmosphere at a constant level. On each day, conductivity-temperature-depth (CTD; SAIV A/S, model SD204) casts monitored the temperature and salinity profiles within the enclosures. The nutrient-initiated bloom was monitored over a 19-day period, during which samples and profiles were taken on a daily basis before midday (0900–1000 h). Samples were taken from 0.5 m depth by gentle vacuum pumping of a 20-liter volume. Immediately after arrival to the onshore laboratory, subsamples for the different analyses were taken. At the end of the experiment, we sampled the material, which settled during the experiment, from mesocosms 1, 4, and 7 by pumping 6 liters of water from the bottom of the enclosures and discarding the first 3 liters.

Measurements and analyses—An overview of all variables determined during the study is given in Table 1. Methods for the determination of variables, which are also included in separate papers, are described only briefly.

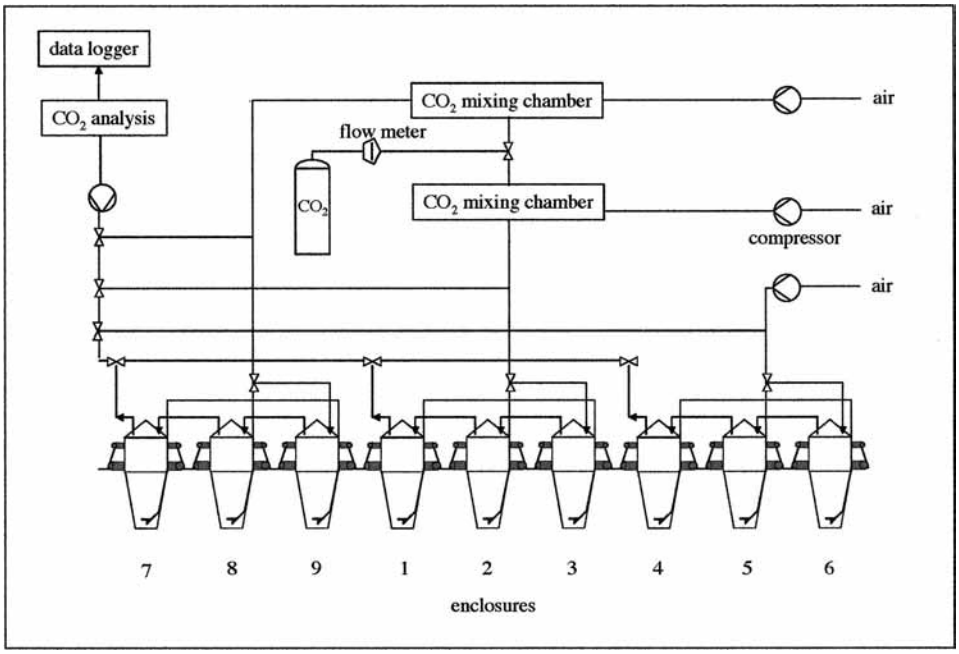

Fig. 1. Schematic representation of the aeration systems for CO_2 manipulation of seawater inside the mesocosms. Surrounding air was either pumped directly to the mesocosms (present mesocosms 4–6) or enriched with CO_2 in a mixing chamber (high-CO_2 mesocosms 1–3), or depleted in CO_2 through adsorption onto Na_2CO_3 platelets (low-CO_2 mesocosms 7–9). The air was injected into the water just above the bottom of the mesocosms, where it was released through a pipe system equipped with a nozzle at its end. To fumigate the atmosphere within the tents, all mesocosms of one treatment were connected. The CO_2 concentration of the air used for aeration of water and atmosphere was measured regularly by a CO_2 gas analyzer.

Irradiance was continuously measured every 10 min throughout the study with a Li-Cor cosine sensor (LI-192SA), mounted on top of the floating mesocosm laboratory. Depth profiles of irradiance inside the mesocosms (on average every 3 d) were measured with a Li-Cor spherical sensor (LI-193SA). The atmospheric pCO_2 inside the tents were monitored up to three times a day by a multicomponent continuous gas analyzer (Rosemount analytical BINOS 100 2M) connected to a portable compact gas conditioning unit (MandC Products PSS-5). The pCO_2 in seawater was measured by means of an equilibrator (Frankignoulle et al. 2001) coupled to an infrared analyzer (Li-Cor 6262). The system was calibrated routinely with air standards with nominal mixing ratios of 0, 350, and 800 ppmV of CO_2 (Air Liquide Belgium and Hydrogas). Temperature at the inlet of the pump and in the equilibrator was measured simultaneously with a Li-Cor thermosensor. For each measurement of CO_2, samples for TA were taken. TA was measured by the classical Gran electrotitration method (Gran 1952) on 100-ml GF/C-filtered samples. The reproducibility of measurements was 3 μmol kg^{-1}. The pCO_2 was then corrected for temperature changes with TA and the dissociation constants of Roy et al. (1993). DIC was calculated from seawater pCO_2 and TA. For both DIC computation and CO_2 temperature compensation, CO_2 speciation was calculated with the use of the CO_2SYS Package (Lewis and Wallace 1998), the CO_2 acidity constants of Roy et al. (1993), the CO_2 solubility coefficient of Weiss (1974), and the borate acidity constant of Dickson (1990). The total borate molality was calculated with the Uppström (1974) ratio to salinity. The uncertainty on the DIC computation is estimated to be 5 μmol kg^{-1}. The pCO_2 of seawater was normalized to a temperature of 12°C (error 3 μmol CO_2).

Chlorophyll *a* (Chl *a*) was determined on 100-ml samples filtered on 0.45-μm cellulose nitrate filters, frozen and extracted in 90% acetone at 4°C overnight as described by Parsons et al. (1984). Chl *a* concentration was measured with a Turner Design Fluorometer (model 10-AU). A standard solution of pure Chl *a* was used for calibration. Nitrate and nitrite were determined from GF/F-filtered and preserved (0.1% $HgCl_2$) samples with an autoanalyzer (AA II) within 4 months. Phosphate and ammonium were measured on the day of sampling by the methods of Koroleff and Grasshof (1983). Total particulate carbon (TPC) and particulate organic nitrogen (PON) were determined by elemental analysis from 1 liters (days 0–12) or 0.5 liter (days 13–19) samples filtered gently (200 mbar) through precombusted (24 h, 500°C) glass fiber filters (GF/F, Whatman). Particulate inorganic carbon (PIC) was determined by subtracting particulate organic carbon (POC) from TPC. For determination of POC, filters were fumed for 2 h with saturated HCl to remove all particulate inorganic carbon and dried for 2 h at ~50°C. TPC, POC, and PON were subsequently measured on a Europa Scientific ANCA SL 20-20 mass spectrometer. Particulate organic phosphorus (POP) was determined colorimetrically (Koroleff and Grasshof 1983) after persulfate

Table 1. Biological and chemical variables determined during the mesocosm study.

Variable	Method	Reference
Algal cell density	Flow cytometry	This study
Alkalinity	Gran electrotitration	Delille et al. unpubl. data
Alkenone concentration	Gas chromatography	A. Benthien unpubl. data
Alkenone $\delta^{13}C$	GCirmMS	A. Benthien unpubl. data
Bacterial abundance	Microscopy	Rochelle-Newall et al. 2004
^{14}C primary production	Radiography	Delille et al. unpubl. data
Chromophonic DOM	Spectrophotometry	Rochelle-Newall et al. 2004
Chl *a*	Fluorometry	This study
Coccosphere/coccolith size	SEM	This study
Coccolith weight	Image analysis	This study
pCO_2	Infrared analyzer (Li-Cor_7 6262)	Delille et al. unpubl. data
DOC	Shimadzu TOC analyzer	Engel et al. 2004*a*
DIC	Calculated from TA, pH, and CO_2	Delille et al. unpubl. data
Light intensity	Li-Cor spherical sensor (LI-193SA)	This study
Mono-/polysaccharides	Colorimetric analysis with TPTZ	Engel et al. 2004b
Net primary production	Winkler titration	Delille et al. unpubl. data
Nutrients	Autoanalyzer	This study
O_2	Winkler titration	Delille et al. unpubl. data
pH	Sensor	This study
PIC	CHN analyzer (TPC-POC)	This study
POC	CHN analyzer	This study
PON	CHN analyzer	This study
POP	Acid combustion	This study
$\delta^{13}C$ POC	Mass spectrometry	Riebesell, unpubl.
Salinity	CTD	This study
Temperature	CTD	This study
TEP	Colorimetric analysis, microscopy	Engel et al. 2004*a*
Viral density	Flow cytometry	Rochelle-Newall et al. 2004

oxidation from 0.5–1.0-liter samples filtered onto GF/F filters. All filters were prepared in duplicate and stored at −20°C until analysis.

Phytoplankton counts were performed with a FACSCalibur flow cytometer (Becton Dickinson) equipped with an air-cooled laser, providing 15 mW at 488 nm, and with a standard filter setup. The cells were analyzed from fresh samples at high flow rate (~70 μl min^{-1}) with the addition of 1-μm fluorescent beads (Molecular Probes). Autotrophic groups were discriminated on the basis of their forward or right angle light scatter (FALS, RALS) and chlorophyll (and phycoerythrin for *Synechococcus* and cryptophyte populations) fluorescence. Listmode files were analyzed with CYTOWIN (Vaulot 1989). The sizes of coccoliths and coccospheres of *E. huxleyi* were determined by scanning electron microscopy (JEOL JSM 6300 SEM). Samples were taken from mesocosms 1, 4 and 7 at days 13, 15, and 17. Every sample (20 ml) was filtered on a 47-mm aerosol-grade 0.4-μm pore-size Nuclepore filter. To enhance the homogeneity of the particle distribution, a paper filter was placed underneath the Nuclepore filter during filtration. Every filter was rinsed three times with 0.05-μmol L^{-1} NH_4HCO_3 buffer to remove crystallized salts. The filters were placed in petri dishes and air dried. Samples were coated with a 50-nm carbon layer to prevent charging during the analysis. From every sample, 200 coccoliths and 200 coccospheres of *E. huxleyi* were measured for their size, calculated as the equivalent spherical diameter from measurements of the coccolith area. The weight of coccoliths sampled on days 0, 4, 9, 11, 14, and 16 from each of the mesocosms was determined by a morphometric method. For this, 1 liter was filtered on cellulose Micronsep (MSI) membrane (0.45 μm effective pore size, 47 mm diameter). The membrane was cut and mounted between slide and coverslip with Canadian Balsam. The slides were scanned by an automatic light microscope (Leica DMRBE) at ×500 magnification with cross-polarized light. One hundred view fields were randomly grabbed by a digital camera and analyzed by SYRACO (Dollfus and Beaufort 1999). On average, 1,800 coccoliths of *E. huxleyi* per sample were recognized. Because coccoliths are made of calcium carbonate, they appear bright in cross-polarized light. The brightness of a thin birefringent calcite object in cross-polarized light depends on its thickness. By measuring the total brightness (the sum of the gray value of all pixels composing the coccolith image), the weight of a coccolith was determined by a transfer function between brightness and calcite weight, derived from pure calcite of known thickness (Beaufort unpubl.).

Statistical treatment of data—Average values are given by the statistical mean ($\bar{x}$) and its standard deviation (SD). Mean values were compared by means of a *t*-test. Significance of the correlation coefficient (r^2) against H_0: $\rho = 0$ was tested by a Student's *t*-test according to Sachs (1974):

$$\hat{t} = \frac{r\sqrt{n-2}}{\sqrt{1-r^2}} \quad (1)$$

Degree of freedom is $n - 2$. H_0 ($r^2 = 0$) is rejected for $\hat{t} \geq \hat{t}_{n-2}$; p. The influence of the CO_2 treatment on biological or chemical variables was determined by means of the analysis of variance. The effect of the CO_2 treatment on a linear relationship between two biological or chemical variables was tested by comparing the slope (b) of the linear regression $F(x) = b(x) + a$, calculated for each treatment separately, with a t-test (Sachs 1974).

$$\hat{t} = \frac{|b_1 - b_2|}{\sqrt{\frac{S^2_{y_1x_1}(n_1 - 2) + S^2_{y_2x_2}(n_2 - 2)}{n_1 + n_2 - 4}\left(\frac{1}{Q_{x_1}} + \frac{1}{Q_{x_2}}\right)}} \quad (2)$$

Degree of freedom is $n_1 + n_2 - 4$. Q_x is the sum of the squared residuals of x, and S_{yx} is the residual variance of y. $H_0(b_1 = b_2)$ is rejected for $\hat{t} \geq \hat{t}_{n_1+n_2-4}$; p. Significance level of each test was $p < 0.05$.

Results

The physical environment—Day length during the study period was between 20.3 and 22.7 h and increased from the beginning of the study until day 15 (midsummer). Average photosynthetically active radiation (PAR) during daytime was 598 ± 213 μmol photons m^{-2} s^{-1} and ranged from 127 to 836 μmol photons m^{-2} s^{-1}. Irradiance at 3.5 m depth inside the mesocosms was always above 1% of surface irradiance. Water temperature increased steadily over the course of the experiment from ~10°C at day 0 to ~13°C at day 19. Daily CTD casts showed virtually no variation of salinity with depth and only minor temperature variation (<0.2°C), indicating even, vertical mixing of the nonparticulate parameters in the mesocosms.

General bloom development—At the beginning of the experiment, seawater pCO_2 was adjusted to 713 ± 6.0 ppmV in the high-pCO_2 scenario of mesocosms 1–3, to 414 ± 11 ppmV in the present-pCO_2 mesocosms 4–6, and to 190 ± 2.4 ppmV in the low-pCO_2 mesocosms 7–9. Because of biological activity, seawater pCO_2 decreased strongly during bloom development (Fig. 2a). This was most pronounced in the high-pCO_2 treatment, largely because of the lower buffering capacity of the carbonate system at higher pCO_2. Parallel to the decrease in pCO_2, the pH of seawater increased in all treatments by 0.27 ± 0.04, 0.18 ± 0.04, and 0.12 ± 0.03 units in the high-, present-, and low-pCO_2 treatments, respectively (Fig. 2b). The decrease in DIC by organic carbon fixation (i.e., the decrease in total DIC minus the amount of inorganic carbon removed through calcification: $\Delta[DIC^*] = [\Delta DIC] - [½\Delta TA]$) was similar in the three treatments and amounted to 161 ± 10 μmol C L^{-1} in the high-pCO_2 mesocosms, to 168 ± 28 μmol L^{-1} in the present-pCO_2 mesocosms and to 156 ± 32 μmol L^{-1} in the low-pCO_2 mesocosms. Detailed information about the changes in the seawater carbonate chemistry during the bloom will be given elsewhere (Delille unpubl.).

Net growth of the phytoplankton community was detectable after day 5 in all of the mesocosms and induced an increase in Chl *a* concentration from about 1 μg L^{-1} prebloom concentration to values between 6.5 and 12.5 μg L^{-1} at the height of the bloom on day 14 (Fig. 3). Thereafter, Chl *a* concentration declined steadily and became more variable between mesocosms. The decline of the phytoplankton bloom was accompanied by particle aggregation, leading to the appearance of amorphous marine snow on day 16.

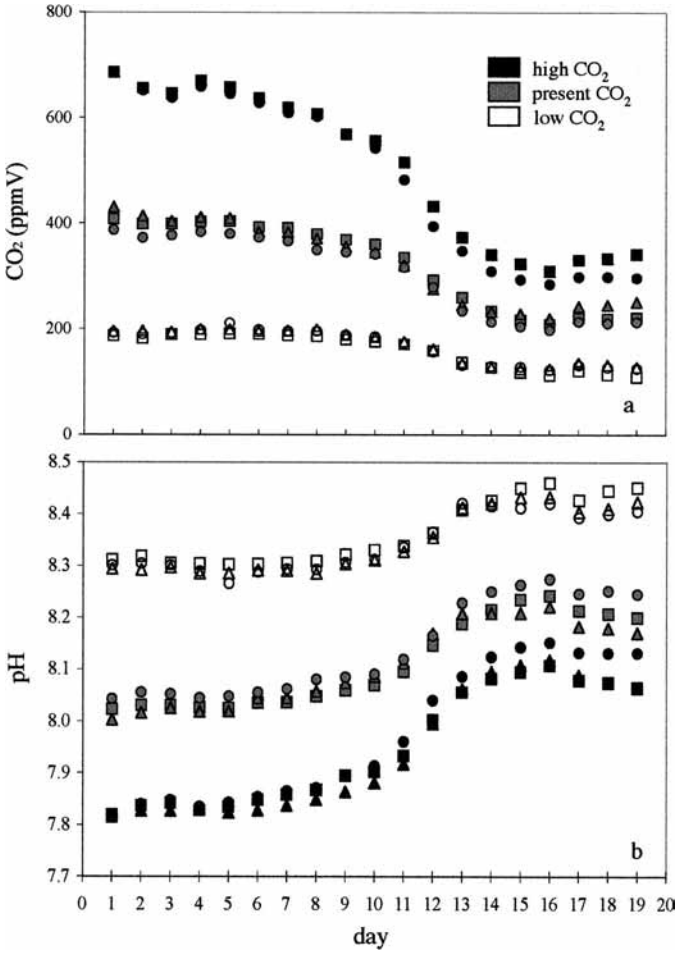

Fig. 2. (a) Changes in seawater pCO_2 and (b) pH occurred in the course of the study in all of the mesocosms and were most pronounced in the high-CO_2 treatment. Black: high-CO_2 treatment; circle, mesocosm 1; square, mesocosm 2; triangle, mesocosm 3. Grey: present-CO_2 treatment; square, mesocosm 4; triangle, mesocosm 5; circle, mesocosm 6. White: low-CO_2 treatment; square, mesocosm 7; triangle, mesocosm 8; circle, mesocosm 9.

During the prebloom and the early exponential growth phase, phytoplankton composition was dominated by number of autotrophic flagellates (mainly *Micromonas* spp.) and picocyanobacteria *Synechococcus* spp. Highest abundance of autotrophic flagellates was observed on day 7, with an average value of 6.7×10^7 cells L^{-1}. *Synechococcus* spp. peaked on day 5, with an average abundance of 1.1×10^7 cells L^{-1}. Both species did not show a response to the CO_2 treatment (ANOVA, $p = 0.51$). The average abundance of *E. huxleyi* in all mesocosms was $0.09 \times 10^6 \pm 0.04 \times 10^6$ cells L^{-1} initially. As the bloom progressed, *E. huxleyi* clearly became the dominant species (Fig. 4). Maximum cell abundance of *E. huxleyi* was reached between days 17 and 18 and varied from 15×10^6 to 56×10^6 cells L^{-1} among

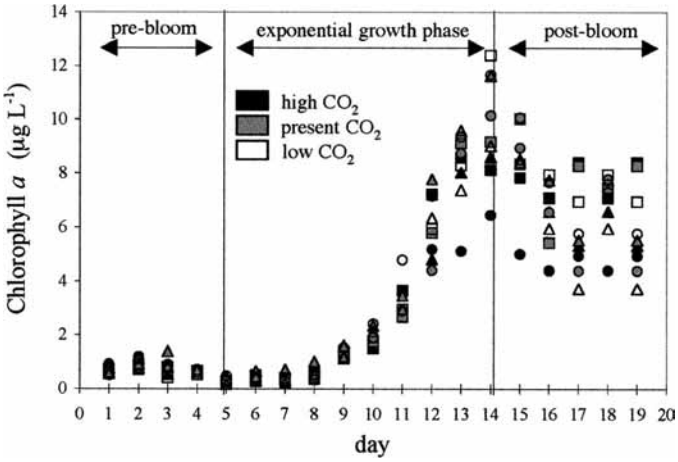

Fig. 3. The development of Chl *a* concentration during the experiment indicated three phases of the phytoplankton bloom: a prebloom phase from days 1 to 5, exponential growth of the phytoplankton from days 5 to 14, when nutrient concentrations were replete, and a postbloom phase after day 14, when nitrate and phosphate were below detection limits. Symbols as in Fig. 2.

all mesocosms (Fig. 5a). Initial PIC concentration was 1.2 ± 1 µmol L^{-1} and increased clearly after day 9 following the course of the *E. huxleyi* population (Fig. 5b). Highest PIC concentrations ranging from 17 to 56 µmol L^{-1} were measured on day 19.

The sizes of coccospheres and of individual coccoliths of *E. huxleyi* were determined on days 13, 15, and 17 by scanning electron microscopy (SEM; Fig. 6). Because only one mesocosm was sampled from each treatment (mesocosms 1, 4, and 7), no information can be given on the variability of coccosphere and coccolith sizes within the CO_2 treatments. Nevertheless, a large number of individual size measurements (n = 600 for each treatment) indicated that the size of coccospheres was significantly different between the treatments (ANOVA, $p < 0.001$). Thereby, the average coccosphere size was significantly larger in the low-pCO_2 mesocosm, at 5.90 ± 0.47 µm, than in the present- and high-pCO_2 mesocosms, at 5.75 ± 0.46 and 5.72 ± 0.61, respectively (t-test, $p < 0.001$). Furthermore, the average sizes of individual coccoliths in the three different mesocosms were 3.58

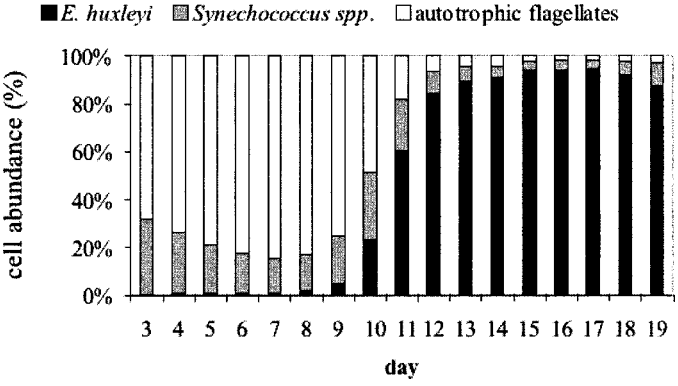

Fig. 4. Mean relative abundance of the major phytoplankton species during the study period.

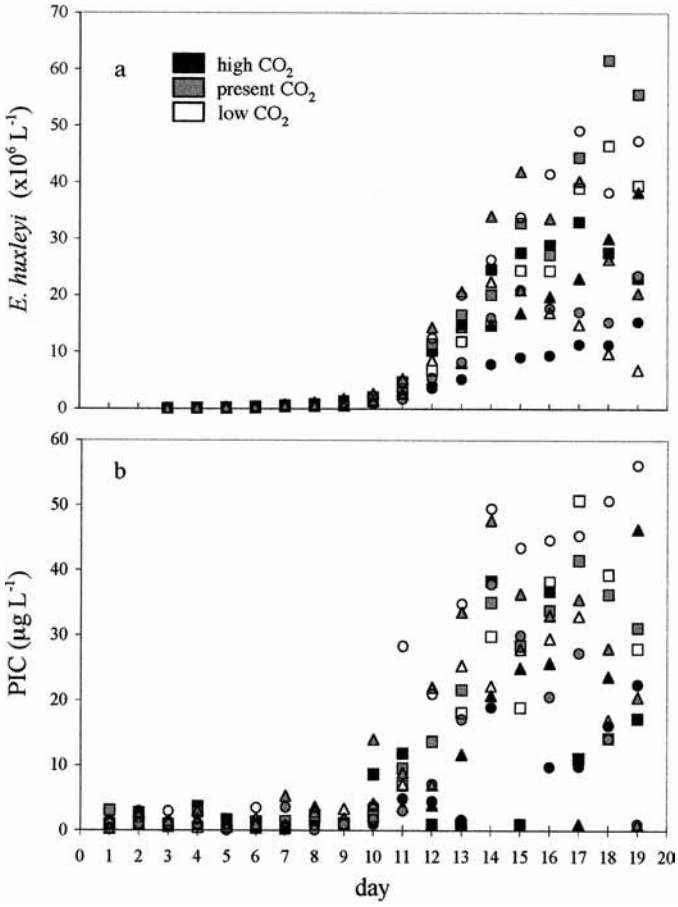

Fig. 5. (a) Growth of the *E. huxleyi* population was accompanied by (b) an increase of particulate inorganic carbon (PIC). Symbols as in Fig. 2.

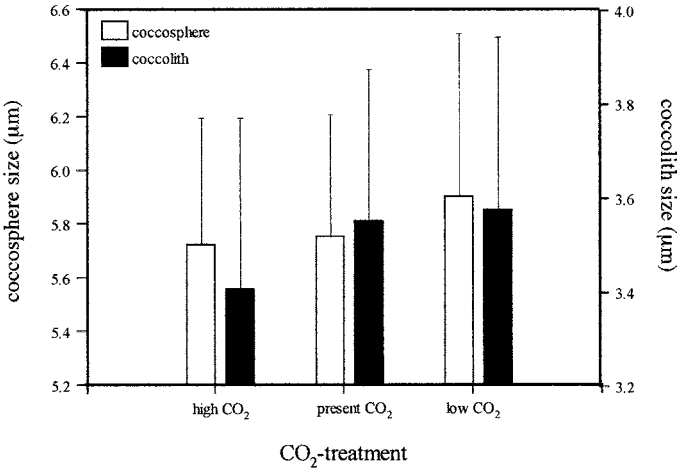

Fig. 6. Average size of coccospheres and coccoliths of *E. huxleyi* determined by SEM from samples of mesocosms 1, 4, and 7 collected on 3 days during the bloom. Number of measurements: n = 600 each; error bars = +1 SD.

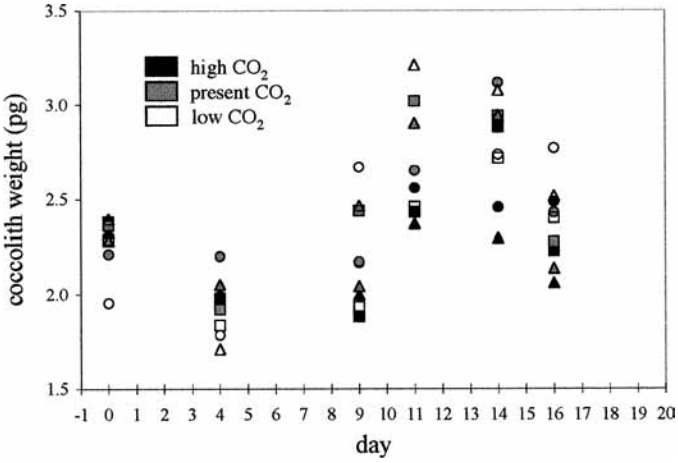

Fig. 7. The weight of *E. huxleyi* coccoliths changed in the course of the bloom. Each data point represents the mean value of at least 1,800 measurements.

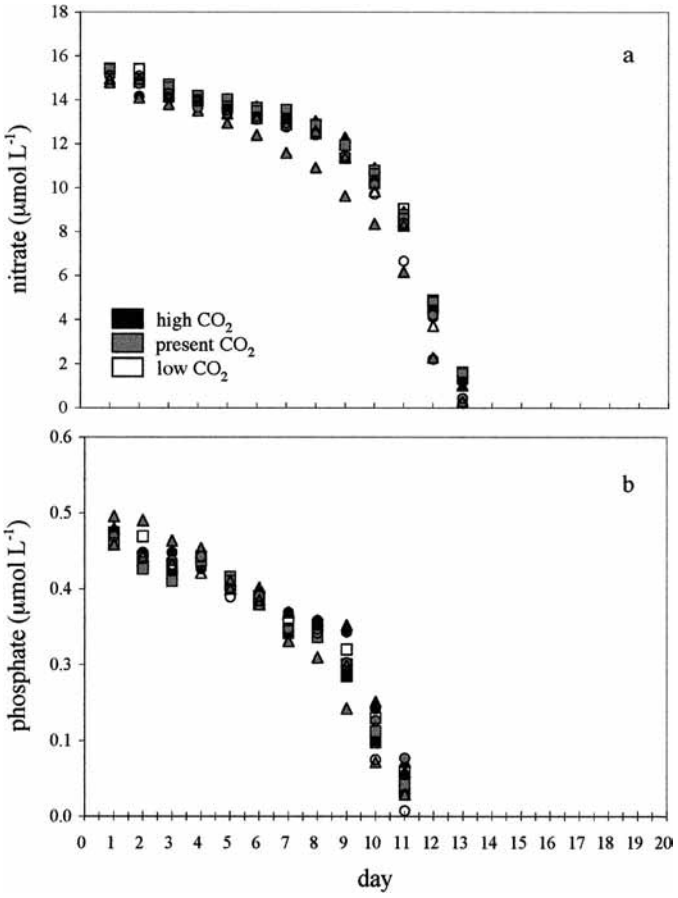

Fig. 8. Biomass growth led to rapid decrease of the inorganic nutrients (a) nitrate and (b) phosphate. Nitrate was below detection limit (0.1 μmol L^{-1}) after day 13, phosphate after day 11 (limit 0.05μmol L^{-1}). Symbols as in Fig. 2.

$\pm$ 0.36, 3.55 $\pm$ 0.32, and 3.41 $\pm$ 0.37 μm in the low-, present-, and high-pCO_2 mesocosms, respectively, and significantly different from each other (ANOVA, $p < 0.001$). Again the average size decreased significantly with increasing pCO_2 (*t*-test, $p < 0.001$). No difference in the visual appearance of coccoliths between the pCO_2 treatments was determined by SEM (i.e., coccospheres and coccoliths of *E. huxleyi* in the high-pCO_2 treatment were not excessively malformed).

Changes in coccolith weight occurred in the course of the bloom, yielding the lowest weights on day 4 and the highest weights between days 11 and 14 (i.e., at the height of the exponential growth phase; Fig. 7). Within each treatment, no relationships between coccolith weight and CO_2 or CO_3 concentration were determined. Between the treatments, significant differences in the weight of *E. huxleyi* coccoliths were observed (ANOVA, $p < 0.001$), with an average coccolith weight of 2.27 $\pm$ 0.25 pg in the high-pCO_2 treatment, which was lower than in the present-pCO_2 treatment at 2.45 $\pm$ 0.37 pg (*t*-test, $p < 0.01$) and also lower than in the low-pCO_2 treatment at 2.45 $\pm$ 0.49 pg (*t*-test, $p < 0.05$).

Cell growth induced a rapid decline of inorganic nutrients after the first week. Nitrate dropped from an initial concentration of 15.3 $\pm$ 0.2 μmol L^{-1} to below the detection limit after day 13 (Fig. 8a). Phosphate started at 0.48 $\pm$ 0.02 μmol L^{-1} and was not detectable after day 11 (Fig. 8b). Ammonium was undetectable during the whole study. Particulate organic phosphorus (POP) and nitrogen (PON) concentrations followed the course of Chl *a* concentration and reached maximum values between days 13 and 14, with 0.2–0.3 μmol POP L^{-1} and 10–12 μmol PON L^{-1} (Fig. 9a,b). PON production ceased directly after nitrate depletion, whereas approximately one third of net POP production occurred within the 2 d after phosphate fell below the detection limit. Average POC concentration was 17.2 $\pm$ 2.0 μmol L^{-1} at the beginning of the study and increased continuously until day 17 (Fig. 9c). Variability of POC concentration among the replicate mesocosms was low initially, but increased after the onset of nutrient depletion, yielding a large range of maximum POC concentrations per mesocosm from 69 to 219 μmol L^{-1} at the end of the study.

Normalization of production rates and elemental stoichiometry—In general, the variability of concentrations of particulate components among the replicate mesocosms was either of equal magnitude or even larger than between the treatments. Hence, no statistically significant differences between the CO_2 treatments were observed during the study regarding absolute concentrations of the particulate components mentioned. However, particle concentration during the course of the bloom was likely affected by small differences in the initial distribution of cells and zooplankton, as well as by secondary processes such as grazing or particle sinking with potentially different rates between the mesocosms. To test whether CO_2 had an effect on the rates of phytoplankton development, the relationships between biological and chemical variables were examined more closely. Whenever possible, a normalization was performed by calculating uptake or production ratios; that is, $(dx/dt)/(dy/dt) = \Delta[x] : \Delta[y]$. The results are listed in Table 2. Because production rates were calculated from changes in standing stocks, the derived ratios address net changes. Particles that settled to the bottom of the mesocosms were not quantified. Elemental ratios of

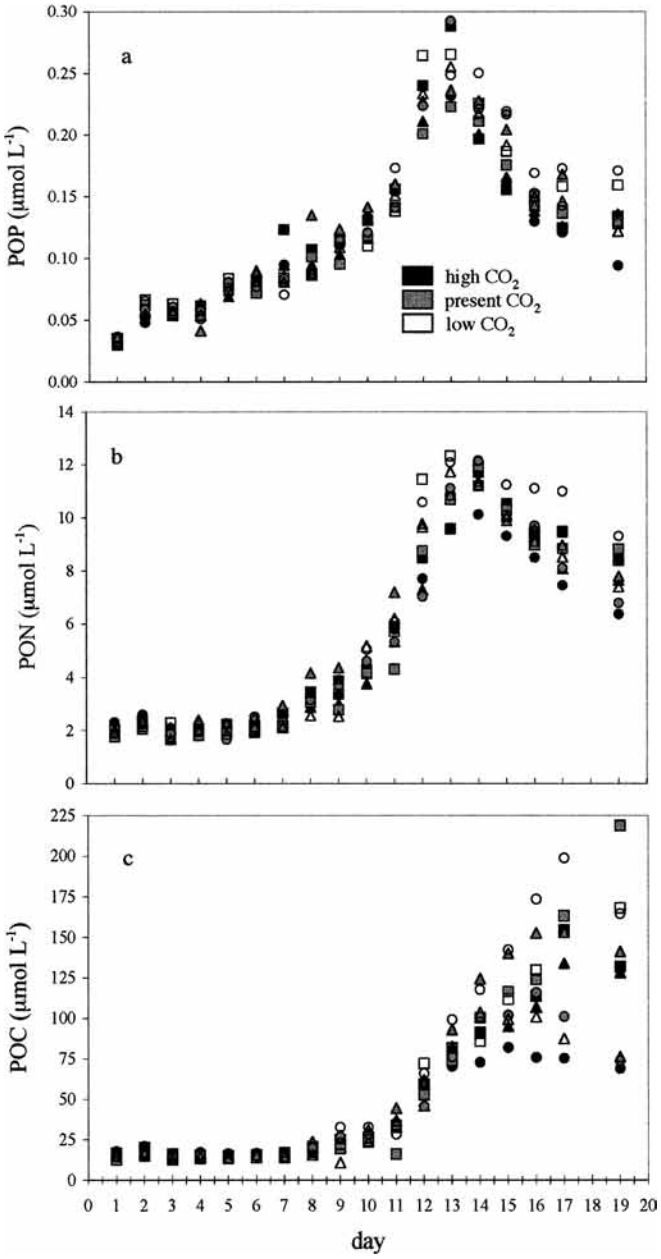

Fig. 9. Development of the particulate organic elements (a) phosphorus (POP), (b) nitrogen (PON), and (c) carbon (POC) in the course of the study. Symbols as in Fig. 2.

particulate matter therefore refer only to the material suspended in the water column.

The net specific growth rate (μ) of *E. huxleyi* was calculated for each treatment as the average of the daily growth rates: $\mu_t = [\ln(C_i) - \ln(C_{i-1})]/[t_i - t_{i-1}]$, with $\ln(C_i)$ and $\ln(C_{i-1})$ being the natural logarithms of cell concentrations on two consecutive days. Until the peak of the bloom (day 14), the net specific growth rate was 0.50 ± 0.26 d^{-1} ($n = 36$) in the low-pCO_2 treatment, 0.47 ± 0.26 d^{-1} ($n = 36$) in the present-pCO_2 treatment, and 0.43 ± 0.19 d^{-1} in the high-pCO_2 treatment ($n = 36$). Although a systematic CO_2 effect on the net specific growth rates of *E. huxleyi* was not determined (ANOVA, $p < 0.1$), the average growth rate in the low-pCO_2 treatment was significantly higher than in the high-pCO_2 treatment (*t*-test, $p < 0.04$). This result is in accordance with a higher net production of PIC relative to POC at low pCO_2 (*t*-test, $p < 0.06$). PIC and POC production were linearly related to *E. huxleyi* cell abundance in all mesocosms (*t*-test, $p < 0.001$). Although Δ[POC]:Δ[Cell] ratios showed no differences between the CO_2 treatments, with an average ratio of 3.9 ± 0.53 pmol cell^{-1}, the Δ[PIC]:Δ[Cell] ratio at low pCO_2 was significantly higher than in the present-pCO_2 treatment (*t*-test, $p < 0.001$) and higher than in the high-pCO_2 treatment. However, because of a large variability of data within the high-pCO_2 treatment, the latter result was of lower significance (*t*-test, $p < 0.06$).

The drawdown of DIC for organic carbon fixation normalized to cell abundance, Δ[DIC*]:Δ[Cell], was highest in the high-pCO_2 treatment (*t*-test, $p < 0.001$), whereas no significant differences in this respect were observed between the present- and the low-pCO_2 treatments. Normalized to nitrate, the drawdown of DIC* uptake until day 13 was significantly higher at high pCO_2 than at present (*t*-test, $p < 0.01$) and low pCO_2 (*t*-test, $p < 0.001$). Thereby, the uptake ratios Δ[DIC*]:$\Delta[NO_3^-]$ in the high- and present-pCO_2 treatments were above the Redfield C:N ratio of 6.6 (Redfield et al. 1963), but below in the low-pCO_2 treatment. In all mesocosms, the net production of Chl *a* was linearly related to the uptake of nitrate ($p < 0.001$) during the exponential growth phase (days 5–13). Thereby, the ratio Δ[Chl *a*]:$\Delta[NO_3^-]$ was lowest at high pCO_2 and significantly different from the respective ratios in the present- and low-pCO_2 treatments ($p < 0.005$).

Despite the higher DIC* uptake, the accumulation of POC decreased as a function of increasing pCO_2. This was indicated by differences in the ratio of POC accumulation to DIC* drawdown, Δ[POC]:Δ[DIC*], which were significant between high and present pCO_2 (*t*-test, $p < 0.001$) and between present and low pCO_2 (*t*-test, $p < 0.05$). Specifically, normalized to the uptake of DIC*, the accumulation of POC was 24% lower in the high-pCO_2 than in the low-pCO_2 treatment. Similar to POC, the accumulation of PON relative to the drawdown of DIC* (i.e., Δ[PON]:Δ[DIC*]) was also significantly smaller at high pCO_2 than at present (*t*-test, $p < 0.001$) and low pCO_2 (*t*-test, $p < 0.001$). The accumulation of POP (i.e., Δ[POP]:Δ[DIC*]) was not significantly different between the high- and present-pCO_2 treatments but was slightly higher in the low-pCO_2 mesocosms (*t*-test, $p < 0.05$).

In accordance with the Δ[DIC*]:$\Delta[NO_3^-]$ uptake ratios, the highest Δ[POC]:Δ[PON] ratios were observed at high pCO_2, significantly higher than those at low pCO_2 ($p < 0.05$), although not significantly different from those in the present-pCO_2 mesocosms. On the contrary, the Δ[POC]:Δ[POP] ratios were lowest in the high-pCO_2 mesocosms (*t*-test, $p < 0.005$). Differences in the elemental stoichiometry of the treatments were also observed for the production of PON relative to POP. Again, high-pCO_2 mesocosm behavior was significantly different from that in the present- and low-pCO_2 mesocosms (*t*-test, $p < 0.001$), having the lowest PON to POP production ratio.

Table 2. The stoichiometry of elements and particles during the bloom was determined by regression analysis of $y = ax + b$. DIC* is the concentration of DIC corrected for changes in alkalinity and salinity. Degree of freedom is $n - 2$. No samples were taken on day 18.

Ratio $\Delta y : \Delta x$ = a	CO_2 treatment	Δt (days)	a	±SD	r^2	df
Δ[DIC*] : Δ[Cell]	High	3–17	−5.5	0.49	0.77	43
(pmol : cell)	Present	3–17	−4.1	0.28	0.84	43
	Low	3–17	−3.6	0.30	0.77	43
Δ[DIC*] : Δ[NO_3]	High	1–13	8.10	0.17	0.98	37
(mol : mol)	Present	1–13	8.11	0.34	0.93	37
	Low	1–13	6.01	0.51	0.78	37
Δ[POC] : Δ[DIC*]	High	1–13	−0.56	0.02	0.95	37
(mol : mol)	Present	1–13	−0.66	0.03	0.92	37
	Low	1–13	−0.74	0.06	0.82	37
Δ[PON] : Δ[DIC*]	High	1–13	-7.4×10^{-2}	0.2×10^{-2}	0.97	37
(mol : mol)	Present	1–13	-8.5×10^{-2}	0.4×10^{-2}	0.94	37
	Low	1–13	-11×10^{-2}	0.7×10^{-2}	0.82	37
Δ[POP] : Δ[DIC*]	High	1–13	-1.9×10^{-3}	8.6×10^{-5}	0.84	37
(mol : mol)	Present	1–13	-1.9×10^{-3}	9.5×10^{-5}	0.86	37
	Low	1–13	-2.0×10^{-3}	20×10^{-5}	0.74	37
Δ[PIC] : Δ[POC]	High	1–19	0.23	0.03	0.60	34
(mol : mol)	Present	1–19	0.24	0.02	0.80	42
	Low	1–19	0.29	0.02	0.84	42
Δ[PIC] : Δ[Cell]	High	3–19	0.94	0.37	0.53	28
(pmol : cell)	Present	3–19	0.84	0.10	0.63	38
	Low	3–19	1.10	0.11	0.76	35
Δ[Chl *a*] : Δ[NO_3]	High	5–13	−0.58	0.03	0.94	25
(μg : μmol)	Present	5–13	−0.66	0.03	0.95	25
	Low	5–13	−0.64	0.02	0.98	24
Δ[POC] : Δ[PON]	High	1–13	7.0	0.2	0.97	37
(mol : mol)	Present	1–13	6.8	0.3	0.95	37
	Low	1–13	6.6	0.3	0.96	37
Δ[POC] : Δ[POP]	High	1–13	260	16	0.87	37
(mol : mol)	Present	1–13	280	21	0.82	37
	Low	1–13	308	19	0.87	37
Δ[PON] : Δ[POP]	High	1–13	37.1	1.9	0.91	37
(mol : mol)	Present	1–13	42.2	2.1	0.92	37
	Low	1–13	47.2	1.8	0.95	37
Δ[PON] : Δ[NO_3]	High	1–13	0.60	0.02	0.98	37
(mol : mol)	Present	1–13	0.67	0.02	0.97	37
	Low	1–13	0.71	0.03	0.95	37

The uptake ratio of nitrate and phosphate was not significantly different between the treatments, yielding a mean $\Delta[NO_3^-] : \Delta[PO_4^{3-}]$ of 15.8 ± 0.41 ($r^2 = 0.94$, $n = 99$). Calculating $\Delta[POP] : \Delta[PO_4^{3-}]$ and $\Delta[PON] : \Delta[NO_3^-]$ ratios revealed that the net yield of phosphorus in POP was similar in all mesocosms but that the net yield of nitrogen in PON decreased with pCO_2 (*t*-test, $p < 0.001$).

In all mesocosms, the phosphorus yield in particulate organic matter was much lower than the nitrogen yield. Hence, the production ratio of Δ[PON] : Δ[POP] differed clearly from the $\Delta[NO_3^-] : \Delta[PO_4^{3-}]$ uptake ratio (Fig. 10). In contrast, the average concentration ratio [PON] : [POP] between days 1 and 14 was 37.5 ± 10 and not differ significantly from the concentration ratio $[NO_3^-] : [PO_4^{3-}]$ between days 1 and 11 at 39 ± 13.

In general, the relationships of POC to PON and POP, respectively, were tight only until nitrate exhaustion on day 13. Thereafter, a decoupling of the dynamics of the nutritional elements occurred, leading to a steep rise of [POC] : [PON] ratios (Fig. 11). As Fig. 11 shows, the behavior of the [POC] : [PON] ratio was independent of the resource ratio $[DIC] : [NO_3^-]$, which increased nonlinearly during the experiment by two orders of magnitude. During the period of nitrate exhaustion, the variability of [POC] : [PON] ratios among the replicate mesocosms increased strongly ($[POC] : [PON]_{\text{days } 14–19}$, $SD_{max} = 5$). As a consequence, the maximum POC concentration of the bloom was neither predictable from PON or nitrate concentrations nor replicable under the same environmental conditions (i.e., within one treatment). Because of the decoupling of elemental dynamics, no rela-

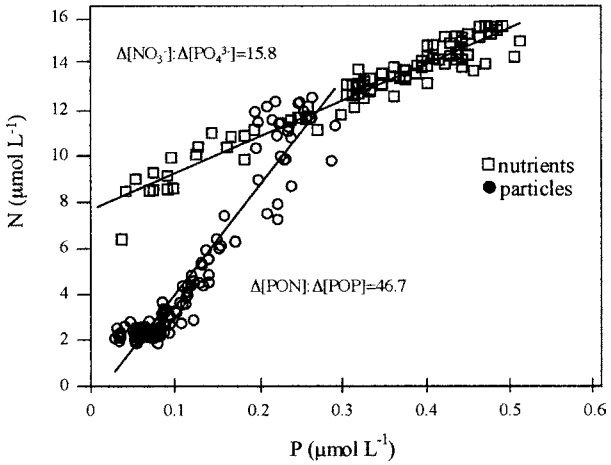

Fig. 10. Differences between the uptake ratio of $[NO_3]:[PO_4]$ and the accumulation ratio of [PON]:[POP] were determined until the height of the bloom (day 14).

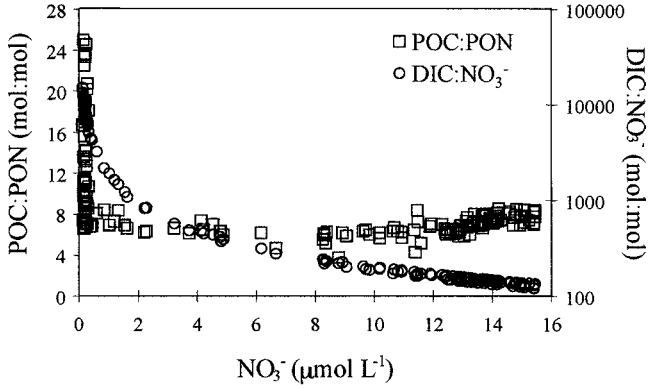

Fig. 11. The ratios of [POC]:[PON] and [DIC]:[NO_3^-] determined from daily samples of all nine mesocosms as a function of nitrate concentration.

tionships between particulate elements existed during the postbloom phase; hence, no CO_2 effects on elemental stoichiometry could be determined for that time.

Discussion

Testing the direct effect of CO_2 concentration and of CO_2-induced changes in seawater carbonate chemistry on natural plankton communities is a difficult task. Sufficiently large differences of CO_2 concentration within a manageable region are difficult to find in the ocean. Our knowledge about the influence of CO_2 on marine phytoplankton therefore stems primarily from laboratory studies and bottle experiments in which CO_2 concentration has been modified either through acid or base addition or has been controlled by aeration. Although these kinds of experiments have the advantage of being highly controllable and reproducible, the dynamics of a natural environment are not well simulated, and important environmental factors, such as particle sinking and zooplankton grazing, are excluded. Moreover, most previous experiments have not addressed the effects of CO_2 on the development and decline of a natural phytoplankton bloom.

To overcome these problems, we have developed an experimental setup that manages and controls the pCO_2 in outdoor seawater mesocosms. The desired CO_2 concentrations representing environments with high, present day, and low CO_2 were achieved within a few days, and perturbation of the chemical equilibrium thereafter was limited to that induced by biological activity within the mesocosm itself. The reproducibility of single components of seawater chemistry within the three replicates of each CO_2 treatment was high, as demonstrated by low variability in pCO_2, pH, alkalinity, and inorganic nutrients within the treatments. By covering the mesocosms with air-tight domes and continuous fumigation of the tents, the CO_2 partial pressure in the overlying air was maintained at a constant level throughout the study. Hence, the experimental setup provided the basic parameters necessary to study the effects of CO_2 changes on a phytoplankton bloom.

During this study, a phytoplankton bloom dominated by the coccolithophorid *E. huxleyi* occurred simultaneously in all of the nine mesocosms. After an initial lag phase of 5 d, exponential growth of the phytoplankton community started, as evidenced in changes in chlorophyll, nutrients, and biomass. This bloom declined after nitrate concentration became exhausted. A postbloom phase characterized by declining Chl *a*, PON, and POP concentrations ensued in the last 5 d of the experiment. When comparing bloom development in the various mesocosms, the most obvious feature was the large variability of particulate concentrations among the replicate mesocosms that obscured clear CO_2 treatment–related effects. Normalization of production rates calculated for the nutrient-replete, exponential growth phase eliminated a large part of natural variability. After nitrate depletion, the biogeochemistry of the bloom became chaotic, in the sense that particulate organic carbon, nitrogen, and phosphorus concentrations were no longer predictable from each other and were highly variable even among the replicates of one treatment (i.e., under the same environmental conditions).

CO_2 treatment–related effects were identified for the growth and calcification rates of *E. huxleyi* and for the stoichiometry of particulate C, N, and P during this study. Calcite formation by *E. huxleyi* was clearly affected by the carbonate chemistry of the seawater and decreased with CO_2 concentration and increased respectively with CO_3 concentration and pH. This was consistently indicated by a variety of measurements showing that in the low-CO_2 treatment (i.e., under lowered CO_2 concentration), the Δ[PIC]:Δ[Cell] and Δ[PIC]:Δ[POC] ratios were highest, the coccospheres and coccoliths largest, and the weight of individual coccoliths highest. These results are furthermore in accordance with an observed decrease in the rate of calcification with increasing CO_2 concentration, as derived from changes in the seawater alkalinity by Delille et al. (unpubl.). Although differences in Δ[PIC]:Δ[POC] ratios could also result from an effect of CO_2 on cell growth and organic carbon production by *E. huxleyi,* the differences in Δ[PIC]:Δ[Cell] ratios and in the size and weight of coccoliths observed between the treatments is direct evidence that calcification itself was affected by the changes of the carbonate chemistry. A direct influence of CO_2-related effects on biological calcification has previ-

ously been demonstrated for corals (Gattuso et al. 1999). This study shows that CO_2 directly affects calcification by *E. huxleyi* during bloom development, as previously suggested in culture studies (Zondervan et al. 2001, 2002).

Another difference between the treatments was detected for the net specific growth rate of *E. huxleyi*, which decreased with pCO_2 and might have influenced differences in net PIC accumulation. Because net specific growth rates were derived from changes in cell concentration, we have to speculate whether cell division rate was directly affected by the CO_2 treatment or whether different loss rates (i.e., by grazing, sinking, or autolysis) occurred. Nitrate and phosphate uptake rate ratios, as well as Chl *a*–normalized ^{14}C-POC primary production rates were similar in all mesocosms (Delille et al. unpubl.) and do not indicate a reduced biomass production at higher CO_2. Reduced calcification rates and direct effects of low pH on cell physiology nevertheless might have affected cell division rates. It has been previously demonstrated that many coastal marine phytoplankton species are directly sensitive to the pH of seawater and that the growth rate of some phytoplankton species has an optimum pH, below and above which the rate of cell division decreases (Hinga 2002). However, bottle experiments with a culture strain of *E. huxleyi* did not show such a decrease of cell growth rates with increasing CO_2 (Zondervan et al. 2002). If we assume that the lower net specific growth rate in the high-CO_2 treatment mirrored cell division rates and was not caused by an enhancement of loss processes, we can conclude that the CO_2 effect on calcification was even stronger than apparent from changes in [PIC] : [POC] ratios. This conclusion is consistent with an earlier study conducted with a culture strain of *E. huxleyi*, which demonstrated that a reduction of growth rates results in increased [PIC] : [POC] ratios (Riegman et al. 2000). Because the opposite was observed during this study (i.e., highest calcification was observed at highest net specific growth rates), the effect of the CO_2 treatment on calcification must have been large enough to counteract and even exceed the growth effect.

The net production of POC and PON relative to the drawdown of DIC* and nitrate, respectively, was significantly affected by CO_2 treatment and decreased with increasing CO_2. Because the Δ[POC] : Δ[POP] and Δ[PON] : Δ[POP] ratios were significantly lower in the high-pCO_2 than in the present- and low-pCO_2 treatments, the data rather point to a selective loss of POC and PON at higher pCO_2 than to reduced cell growth. This loss of carbon and nitrogen has resulted either from an enhanced release of carbon and nitrogen into the dissolved organic matter (DOM) pool or from a higher sedimentation rate of phosphorus-depleted particles. The average increase of DOC was 11 ± 8 μmol C L^{-1}, equal to approximately 18% of the DIC* taken up during the study. Because a significantly different accumulation of DOC between the CO_2 treatments was not detected (Engel et al. 2004*a*), DOC accumulation does not explain the differences in Δ[POC] : Δ[DIC*] ratios between the treatments. Particle sinking was therefore most likely responsible for the differences in the loss of particulate organic elements between the treatments, at least for carbon. The cause of a higher POC sedimentation rate with increasing pCO_2 remains an open question. Although enhanced sedimentation of particles, such as cells and detritus, might have been responsible for the observed differences in net growth rates, an enhanced sedimentation of *E. huxleyi* cells, potentially depleted in phosphorus, at higher pCO_2 cannot fully explain the reduced fraction of POC formation relative to DIC* uptake in these mesocosms. *E. huxleyi*–derived organic carbon accounted for only 32% of POC, assuming a maximum carbon quota of 1.3 pmol $cell^{-1}$, as determined by Zondervan et al. (2001). Net growth rates differed by ~14%, equal to 4.5% of POC. In contrast, differences between POC accumulation normalized to DIC* drawdown were on the order of 16% and 22% of POC. Thus, differences in net growth or loss rates of *E. huxleyi* were not large enough to quantitatively account for the different loss of POC.

An additional POC loss might have been provided by sinking of transparent exopolymer particles (TEP) because the formation rate of TEP normalized to cell abundance was significantly increased in the high-CO_2 mesocosms (Engel et al. 2004*a*). TEP originate from dissolved precursors and are known to favor particle aggregation (Engel 2000). Moreover, because TEP are mainly carbohydrates, they are relatively carbon rich and yield C : N ratios of ~26 (Engel and Passow 2001, Mari et al. 2001). An enhanced formation of TEP at a high CO_2 concentration could have resulted in enhanced aggregation of detrital particles with TEP and, subsequently, in the sedimentation of particles with an increased carbon and nitrogen content but depleted in phosphorus. The formation of aggregates with high TEP content was observed later during the bloom (Engel et al. 2004*a*). However, because of the high variability in particulate components, a statistically significant influence of TEP formation on the C : N ratios of particles could not be determined.

CO_2 effects on the C : N ratio are of special interest in evaluating the potential influence of pCO_2 on the export fluxes of organic carbon in the ocean because export production is considered to be determined by the supply of nitrate to the surface ocean. Until the peak of the bloom, the Δ[DIC*] : $\Delta[NO_3^-]$ uptake ratio was significantly higher under high than under present or low pCO_2. This indicates that the organic carbon yield of the nitrate-based production might increase with pCO_2. Comparing the uptake ratio Δ[DIC*] : $\Delta[NO_3^-]$ with the yield of carbon in particulate matter showed that the loss of POC increased with pCO_2. When comparing the Δ[DIC*] : $\Delta[NO_3^-]$ uptake ratio with the Δ[POC] : Δ[PON] accumulation ratio, we furthermore see that the C : N ratios of uptake processes were higher than the C : N ratios of particle formation under high and present pCO_2, but lower under low-pCO_2 conditions. Thus, an increased carbon uptake at present and high pCO_2 seems to stimulate a preferential loss of carbon, whereas a reduced carbon uptake at low pCO_2 apparently results in a selective accumulation of carbon in particles. It should be noted that the Δ[POC] : Δ[PON] ratio in the low-CO_2 treatment conformed to the Redfield ratio, whereas there was a trend toward higher C : N ratios with increasing pCO_2. Thus, our study indicates that with increasing pCO_2 (1) the rate of particle loss is higher and (2) the elemental composition of sinking particles is shifted toward higher C : N ratios. Specifically, considering that, in the high-pCO_2 treatment, 60% of nitrate drawdown and 56% of DIC drawdown between days

1 and 13 accumulated as PON and POC, respectively (*see* $\Delta[PON]:\Delta[NO_3^-]$ and $\Delta[POC]:\Delta[DIC]$ in Table 2), the loss C : N ratio of carbon and nitrogen in this treatment would have been 8.4. In comparison, the corresponding values in the low-CO_2 treatment would be 71% and 74%, yielding a theoretical loss C : N ratio of 2.4.

No CO_2 effects were determined regarding the total uptake of nitrate and phosphate. For phosphate, this result was not surprising because phosphorus was the least available element and likely to become exhausted in all mesocosms. The drawdown of nitrate relative to phosphate followed Redfield stoichiometry, with an N : P ratio of approximately 16. Because nitrate and phosphate were added at a ratio of 30 : 1, a surplus of nitrate was left at the onset of phosphate exhaustion. The uptake of surplus nitrate and the development of the *E. huxleyi* population after the onset of phosphate exhaustion, as well as the ongoing POP formation between days 11 and 14, indicated the utilization of dissolved organic phosphorus (DOP). It is well documented that under P-limiting conditions, *E. huxleyi* has a high uptake affinity for DOP on the basis of production and release of the ectoenzyme alkaline phosphatase (Riegmann et al. 2000). The average concentration ratio of [N] : [P] in particles until the height of the bloom was similar to those of the inorganic nutrients, which apparently supports the hypothesis that unbalanced nutrient supply (relative to the Redfield ratio) results in unbalanced elemental stoichiometry of cells (Sterner and Elser 2002). However, it should be noted that the uptake ratio of nitrate and phosphate strongly deviated from the production ratio of PON and POP, and rather points to a balanced (i.e., Redfield-like) stoichiometry of growing (nutrient-assimilating) cells and simultaneously degrading POP from detritus. A rapid turnover of phosphorus was further indicated by the observation that apparently only 35% of the phosphorus assimilated as phosphate was stored in suspended particles. Compared with a nitrogen yield of 60–71% in PON, this indicated either sedimentation of POM with a lower N : P ratio than observed for the suspended POM or the release of organic phosphorus to the DOM pool. Sedimentation of relatively phosphorus-rich particles was very unlikely because samples of the sediment taken from the bottom of the mesocosms at the end of the study had a PON : POP ratio of 168 ± 43, clearly above the N : P ratio of suspended particles. Because P exhaustion was likely overcome by the utilization of organic phosphorus resources, nitrate has to be considered the ultimate limiting nutrient and therefore was likely to become depleted in all of the mesocosms.

We used high, present, and low CO_2 concentrations in this experiment, representing the future, present, and glacial atmospheric CO_2 conditions, respectively. Implications of the observed CO_2-related effects for the understanding of changes in the biogeochemistry and ecology of phytoplankton blooms between glacial and future times should, however, be interpreted with caution. To identify the direct effect of CO_2 on the *E. huxleyi* bloom, it was necessary to keep all other environmental factors comparable among the mesocosms. As mentioned before, the oceanographic and chemical condition of the ocean does not remain steady from glacial to future times. Moreover, the response to the combined effects of global change (e.g., CO_2 and temperature) could be different in magnitude than the response to changing CO_2 concentration alone (Reynaud et al. 2003). However, because of its high heat capacity and huge mass, relative changes in ocean surface temperatures on a global scale are proportionately smaller than the changes in surface ocean chemistry from the uptake of CO_2. Moreover, the continuous increase in CO_2 concentration represents a change beyond the range of seasonal or spatial variability of environmental factors phytoplankton species usually encounter in the ocean. Nevertheless, to provide a detailed and realistic picture of global change for the marine ecosystem, the multiple effects of environmental change need to be addressed. The design and management of experiments that can cope with one or more variable factors, in addition to CO_2, while maintaining a natural environment will be a challenging task for oceanography in the future.

It has been suggested that a decrease in the ratio of PIC : POC in sinking material could significantly affect the ocean's capacity to store atmospheric CO_2, potentially acting as a negative feedback to increasing atmospheric CO_2 concentrations (Riebesell et al. 2000; Zondervan et al. 2001). This study supports the earlier observation of reduced calcification rates at high CO_2 concentrations and the conclusion that the carbonate pump could be particularly sensitive to CO_2-related changes in seawater chemistry. The PIC : POC ratio of the sinking particles (i.e., the rain ratio) was not determined during this study but might have been even lower than the respective ratio in the suspended particles because of the suggested higher loss of POC at high pCO_2. Moreover, if the reduction of the net specific growth rate of *E. huxleyi* is indeed representative of the natural environment under high CO_2, the ability of this species to compete with other algae might become affected in the future. A community shift toward noncalcifying phytoplankton species could not only induce changes in the alkalinity of the ocean, as suggested by Riebesell et al. (2000), but could also reduce the amount of export production, which is correlated with $CaCO_3$ fluxes below 1,000 m water depth (Armstrong et al. 2002; Klaas and Archer 2002; Barker et al. 2003). On the other hand, if the observed differences in the loss of POC were associated with an enhancement of TEP-driven aggregation processes, the mode of sedimentation could shift toward a higher rate of aggregate sinking. A higher proportion of aggregates would increase the average sinking velocity of POM and, hence, increase the remineralization depth of POM, which in turn would lead to a deeper export of primary production.

We did not deal with any influence of pCO_2 changes on the heterotrophic food web during this study, apart from determining bacterial abundances, which were not different between the treatments (Rochelle-Newall et al. 2004). However, because the growth efficiency of heterotrophic organisms is controlled by the quality of food, the observed differences in the elemental stoichiometry of particle formation suggests that CO_2 could indirectly affect heterotrophic processes, such as growth rate, particle decomposition, and nutrient recycling.

Our study suggests that *E. huxleyi* is indeed sensitive to changes in CO_2 concentration, as was concluded from chang-

es in net specific growth rates and the calcification of cells, as well as from changes in the stoichiometry of elemental uptake, accumulation, and loss processes. This means that in addition to the expected indirect effects, changes in CO_2 concentration could directly influence biogeochemical cycling and carbon export in the ocean, as well as food web dynamics. To evaluate the direct effects of CO_2 concentration on export production, future studies will need to obtain information about the rates and timing of particle sinking, as well as about the elemental composition of the exported material.

References

ARMSTRONG, R. A., C. LEE, J. I. HEDGES, S. HONJO, AND S. G. WAKEHAM. 2002. A new, mechanistic model for organic carbon fluxes in the ocean based on the quantitative association of POC with ballast minerals. Deep-Sea Res. II **49:** 219–236.

BADGER, M. R., T. J. ANDREWS, S. M. WHITNEY, M. LUDWIG, D. C. YELLOWLEES, W. LEGGAT, AND G. D. PRICE. 1998. The diversity and coevolution of Rubisco, plastids, pyreniods, and chloroplast-based CO_2-concentrating mechanisms in algae. Can J. Bot. **76:** 973–1002.

BARKER, S., J. A. HIGGINS, AND H. ELDERFIELD. 2003. The future of the carbon cycle: review, calcification response, ballast and feedback on atmospheric CO_2. Philos. Trans. R. Soc. Lond. Ser. A361. **1810:** 1997–1999.

BREWER, P. G., C. GOYET, AND G. FRIEDERICH. 1997. Direct observation of the oceanic CO_2 increase revisited. Proc. Natl. Acad. Sci. USA **94:** 8308–8313.

BURKHARDT, S., G. AMOROSO, U. RIEBESELL, AND D. SÜLTEMEYER. 2001. CO_2 and HCO_3-uptake in marine diatoms acclimated to different CO_2 concentrations. Limnol. Oceanogr. **46:** 1378–1391.

———, I. ZONDERVAN, AND U. RIEBESELL. 1999. Effect of CO_2 concentration on C : N : P ratio in marine phytoplankton: a species comparison. Limnol. Oceanogr. **44:** 683–690.

CALDEIRA, K., AND M. E. WICKETT. 2003. Anthropogenic carbon and ocean pH. Nature **425:** 365.

CHEN, G.-T., AND F. J. MILLERO. 1979. Gradual increase of oceanic CO_2. Nature **277:** 205–206.

DICKSON, A. G. 1981. An exact definition of total alkalinity and a procedure for the estimation of alkalinity and total inorganic carbon from titration. Deep-Sea Res. **28:** 609–623.

———. 1990. Thermodynamics of the dissociation of boric acid in synthetic seawater from 273.15 to 318.15 K. Deep-Sea Res. **37:** 755–766.

DOLLFUS, D., AND L. BEAUFORT. 1999. Fat neural network for recognition of position-normalised objects. Neural Networks **12:** 553–560.

DUGDALE, R. C., AND J. J. GOERING. 1967. Uptake of new and regenerated forms of nitrogen in primary productivity. Limnol. Oceanogr. **12:** 196–206.

EGGE, J. K., AND D. L. AKSNES. 1992. Silicate as regulating nutrient in phytoplankton competition. Mar. Ecol. Prog. Ser. **83:** 281–289.

ENGEL, A. 2000. The role of transparent exopolymer particles (TEP) in the increase in apparent particles stickiness (α) during the decline of a diatom bloom. J. Plankton Res. **22:** 485–497.

———. 2002. Direct relationship between CO_2-uptake and transparent exopolymer particles (TEP) production in natural phytoplankton. J. Plankton Res. **24:** 49–53.

———, B. DELILLE, S. JACQUET, U. RIEBESELL, E. ROCHELLE-NEWALL, A. TERBRÜGGEN, AND I. ZONDERVAN. 2004*a*. TEP and DOC production by *Emiliania huxleyi* exposed to different CO_2 concentrations: a mesocosms experiment. Aquat. Microb. Ecol. **34:** 93–104.

———, AND U. PASSOW. 2001. The carbon and nitrogen content of transparent exopolymer particles (TEP) derived from diatom exudates. Mar. Ecol. Prog. Ser. **219:** 1–10.

———, S. THOMS, U. RIEBESELL, E. ROCHELLE-NEWALL, AND I. ZONDERVAN. 2004*b*. Polysaccharide aggregation as a potenial sink for marine dissolved organic carbon. Nature **428:** 929–931.

EPPLEY, R. W., AND B. J. PETERSON. 1979. Particulate organic matter flux and planktonic new production in the deep ocean. Nature **282:** 677–680.

FRANKIGNOULLE, M., A. V. BORGES, AND R. BIONDO. 2001. A new design of equilibrator to monitor carbon dioxide in highly dynamic and turbid environments. Water Res. **35:** 1344–1347.

GATTUSO, J.-P., D. ALLEMAND, AND M. FRANKIGNOULLE. 1999. Photosynthesis and calcification at cellular, organismal and community levels in coral reefs: a review on interactions and control by carbonate chemistry. Am. Zool. **39:** 160–183.

GERVAIS, F., AND U. RIEBESELL. 2001. Effect of phosphorus limitation on elemental composition and stable carbon isotope fractionation in a marine diatom growing under different CO_2 concentrations. Limnol. Oceanogr. **46:** 497–504.

GOERIKE, R., AND B. FRY. 1994. Variations of marine plankton δ13C with latitude, temperature, and dissolved CO_2 in the world ocean. Glob. Biogeochem. Cycles **8:** 85–90.

GRAN, G. 1952. Determination of the equivalence point in potentiometric titration, part ll. Analyst **77:** 661–671.

HINGA, K. R. 2002. Effects of pH on coastal marine phytoplankton. Mar. Ecol. Prog. Ser. **238:** 281–300.

HOUGHTON J. T., AND OTHERS. 2001. Climate change 2001: the scientific basis: contribution of working group I to the third assessment report of the Intergovernmental Panel of Climate Change. Cambridge Univ. Press.

KLAAS, C., AND D. ARCHER. 2002. Association of sinking organic matter with various types of mineral ballast in the deep sea: implications for the rain ratio. Glob. Biochem. Cycles **16**. [doi: 10.1029/2001GB001765]

KOROLEFF, F., AND K. GRASSHOF. 1983. Determination of nutrients, p. 125–188. *In* K. Grasshof, M. Erhardt, and K. Kremling [eds.], Methods of seawater analyses. Verlag Chemie.

LEWIS, E., AND D. WALLACE. 1998. CO_2sys Program developed for CO_2 system calculations, ORNL/CDIAC-105. Carbon Dioxide Information Analysis Center, Oak Ridge National Laboratory, U.S. Department of Energy.

MARI, X., S. BEAUVAIS, R. LEMEE, AND M. L. PEDROTTI. 2001. Non-Redfield C : N ratio of transparent exopolymeric particles in the northwestern Mediterranean Sea. Limnol. Oceanogr. **46:** 1831–1836.

PARSONS, T. R., Y. MAITA, AND C. M. LALLI. 1984. A manual of chemical and biological methods for seawater analysis. Pergamon Press, Oxford.

RAVEN, J. A. 1991. Physiology of inorganic C acquisition and implications for resource use efficiency by marine phytoplankton: relation to increased CO_2 and temperature. Plant. Cell Environ. **14:** 779–794.

REYNAUD, S., N. LECLERCQ, S. ROMAINE-LIOUD, C. FERRIER-PAGES, J. JAUBERT, AND J.-P. GATTUSO. 2003. Interacting effects of CO_2, partial pressure and temperature on photosynthesis and calcification in a scleractinian coral. Glob. Change Biol. **9:** 1660–1668.

REDFIELD, A. C., B. M. KETCHUM, AND F. A. RICHARDS. 1963. The influence of organism on the composition of sea-water, p. 26–77. *In* M. N. Hill [ed.], The sea, 2nd ed. Wiley.

RIEBESELL, U., I. ZONDERVAN, B. ROST, P. D. TORTELL, R. ZEEBE, AND F. M. M. MOREL. 2000. Reduced calcification of marine

plankton in response to increased atmospheric CO_2. Nature **407:** 364–367.

RIEGMAN, R., W. STOLTE, A. A. M NOORDELOOS, AND D. SLEZAK. 2000. Nutrient uptake and alkaline phosphatase (APase) activity of *Emiliania huxleyi* (Prymnesiophyceae) during growth under N and P limitation in continuous cultures. J. Phycol. **36:** 87–96.

ROCHELLE-NEWALL, E., AND OTHERS. 2004. Chormophoric dissolved organic matter in experimental mesocosms maintained under different pCO_2 levels. Mar. Ecol. Prog. Ser. **272:** 25–31.

ROST, B., U. RIEBESELL, S. BURKHARDT, AND D. SÜLTEMEYER. 2003. Carbon acquisition of bloom-forming marine phytoplankton. Limnol. Oceanogr. **48:** 55–67.

ROY, R., AND OTHERS. 1993. The dissociation constants of carbonic acid in seawater at salinities 5 to 45 and temperatures 0 to 45°C. Mar. Chem. **44:** 249–267.

SACHS, L. 1974. Angewandte Statistik. Springer Verlag.

SCIANDRA, A., J. HARLAY, D. LEFEVRE, R. LEMEE, P. RIMMELIN, M. DENIS, AND J. P. GATTUSO. 2003. Response of coccolithophorid *Emiliania huxleyi* to elevated partial pressure of CO_2 under nitrogen limitation. Mar. Ecol. Prog. Ser. **261:** 111–122.

STERNER, R. W., AND J. J. ELSER (EDS.) 2002. Ecological stoichiometry. Princeton Univ. Press.

TORTELL, P. D., G. R. DITULLIO, D. M. SIGMANN, AND F. M. M. MOREL 2002. CO_2 effects on taxonomic composition and nutrient utilization in an equatorial Pacific phytoplankton assemblage. Mar. Ecol. Prog. Ser. **236:** 37–43.

UPPSTRÖM, L. 1974. The boron-chlorinity ratio of deep seawater from the Pacific Ocean. Deep-Sea Res. **21:** 161–163.

URABE, J., TOGARI, J, AND J. J. ELSER 2003. Stoichiometric impacts of increased carbon dioxide on a planktonic herbivore. Glob. Change Biol. **9:** 818–825.

VAULOT, D. 1989. CytoPC: processing software for flow cytometric data. Signal Noise **2:** 8.

WEISS, R. F. 1974. Carbon dioxide in water and seawater: the solubility of a non-ideal gas. Mar. Chem. **2:** 203–215.

WILLIAMS, P. J. LE B., AND J. K. EGGE. 1998. The management and behaviour of the mesocosms. Est. Coast Shelf Sci. **46:** 3–14.

ZONDERVAN, I., B. ROST, AND U. RIEBESELL. 2002. Effect of CO_2 concentration on the PIC/POC ratio in the coccolithophore *Emiliania huxleyi* grown under light-limiting conditions and different daylengths. J. Exp. Mar. Biol. Ecol. **272:** 55–70.

———, R. E. ZEEBE, B. ROST, AND U. RIEBESELL. 2001. Decreasing marine biogenic calcification: a negative feedback on rising atmospheric pCO_2. Glob. Biogeochem. Cycles **15:** 507–516.

Received: 3 February 2004
Amended: 15 November 2004
Accepted: 15 November 2004